Soot Volume Fraction Profiling of Asymmetric Diffusion Flames through Tomographic Imaging

Md. Moinul Hossain, Gang Lu* and Yong Yan
School of Engineering and Digital Arts, University of Kent, Canterbury, Kent CT2 7NT, UK
mmh22@kent.ac.uk, g.lu@kent.ac.uk and y.yan@kent.ac.uk

Abstract- **This paper presents the 3-D (three-dimensional) reconstruction of soot volume fraction of diffusion flames based on tomographic imaging and image processing techniques. Eight flexible imaging fiber bundles and two RGB (Red, Green and Blue) CCD (Charge-coupled Device) cameras are used to obtain concurrently the 2-D (two-dimensional) image projections of the flame from eight different angles of view around the burner. Algorithms which combine the tomographic and two-color pyrometric techniques are utilized to reconstruct the soot volume fraction distributions on both cross- and longitudinal-sections of the flame. A series of experiments were carried out on a gas-fired combustion rig for the determination of soot volume fraction using the algorithms proposed. Test results demonstrate the effectiveness of the developed algorithms.**

Keywords— Flame monitoring; soot volume fraction; imaging fiber; CCD camera; tomography; two-color pyrometry.

I. INTRODUCTION

The flame characteristics such as temperature and soot volume fraction provide instantaneous information on the flame radiation, heat transfer and particulate emission from combustion [1]. The measurement of the flame soot volume fraction is therefore high desirable for combustion researchers and engineers for an in-depth understanding of soot formation process and subsequently the optimization of combustion process [2]. Various optical techniques [3-7] were used for the 2-D measurements of flame soot volume fraction. In recent years, optical tomographic techniques have been received a great attention for the 3-D measurements of flame soot volume fraction [8]. Such a technique has clear advantages over other optical approaches including simple system set-up, high spatial resolution, and relatively low cost, making it most suitable for the 3-D reconstruction and characterization of flame in practical furnaces [8, 9].

Several single camera based tomographic systems have been developed for the 3-D reconstruction of soot volume fraction [10, 11]. Huang et al. [10] described an imaging system incorporating with a single camera and a stereoscopic imaging adapter for reconstructing soot temperature and volume fraction profiles of a laboratory-scale flame. Veríssimo et al. [11] also used a single-camera based tomographic system for the reconstruction of C_2 and soot distributions of the flame where the flame images were captured by the camera rotated from several angular directions. The single-camera approach is relatively simple, but it can only be used under strict conditions where the flame is steady and has a high level of rotational symmetry. A few of multi-camera based tomographic systems has been reported for the 3-D reconstruction of flame soot volume fraction [12, 13]. Legros et al. [12] used three CCD cameras for estimating the soot volume fraction distribution in a laminar diffusion flame. Liu et al. [13] developed four CCD cameras based tomographic system for the 3-D measurement of soot temperature and volume fraction distribution in both axisymmetric and asymmetric flames. Although the multi-camera approach offers a more accurate measurement, the increased number of cameras and optics (e.g., mirrors and lenses) result in a high complexity of system configuration in addition to a high capital cost. It has also been noted that, in the existing multi-camera systems, the number of image projections are still very limited (up to four), resulting in a limited accuracy in the reconstruction of soot volume fraction, particularly for asymmetric flames. There is therefore still a need to develop a more advanced hardware and software platform for spatial and temporal reconstruction of the soot temperature and volume fraction of flames.

This paper presents an algorithm, incorporating with optical tomographic and image processing techniques, for the reconstruction of the soot volume fraction of asymmetric diffusion flames. 2-D images of flame are captured at eight different angles of view around the burner using an optical tomographic system [9]. The gray-levels of the two primary color images of flame are reconstructed using the combined LFBP (logical filtered back-projection) and SART (simultaneous algebraic reconstruction techniques) algorithm. The soot volume fraction distribution of flame is then determined based on two-color pyrometry and soot radiation theories. Experimental results on a gas fired combustion test rig are also reported and discussed.

II. METHODOLOGY

Fig. 1 shows the schematic diagram of the reconstruction of soot volume fraction of a flame. The optical tomographic system which was previously developed [9] was utilized to obtain the 2-D images of the flame. The system mainly consists of two RGB (Red, Green and Blue) CCD cameras (with an image resolution of 1024(H)×768(V) and a frame rate of 25

This work is supported by the Research Council UK (RCUK)'s Energy Programme (EP/G062153/1). The Energy Programme is an RCUK cross-council initiative led by EPSRC and contributed to by ESRC, NERC, BBSRC and STFC.

* Corresponding author: Tel: +44(0)1227823706; Fax: +44(0)1227456084

frames per second), coupling with eight imaging fiber bundles (each having 30k individual fibers and a 92° objective lens). The imaging fiber bundles are arranged around one side of the burner with an angle of 22.5° between two adjacent bundles, transmitting concurrently 2-D images of a flame from eight different angles of view into the two cameras (each camera takes four images from the fiber bundles). The arrangement of eight image projections is considered to be a trade-off between the complexity of the system and the accuracy of the image reconstruction. However, performing the tomographic reconstruction of the flame based on the limited number (i.e., eight in the study) of independent projections could lead to an underdetermined problem [8]. To overcome the problem, the LFBP-SART (logical filtered back-projection and simultaneous algebraic reconstruction techniques) was employed. The LFBP-SART has shown a possibility of using eight image projections to perform the 3-D reconstruction of a flame with an acceptable resolution and accuracy [9]. More detailed description of the imaging system and tomographic algorithms can be found elsewhere [9, 14].

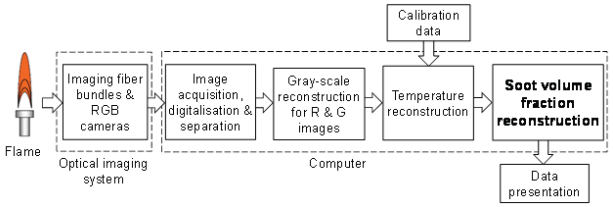

Fig.1. Schematic diagram of the 3-D reconstruction of flame soot volume fraction through tomographic imaging.

To perform the reconstruction of soot volume fraction distribution, the initial task is to reconstruct the gray-level sections of R and G images of each RGB image frame based on the LFBP-SART. Once the gray-level reconstruction of the two color banded images is achieved, the soot temperature can be determined based on the two-color pyrometry [6, 14]. The soot volume fraction, f_v, can then be estimated by [15],

$$f_v = -\frac{\lambda_R}{36\pi F(\lambda_R)L}\ln\left[1-\varepsilon_{\lambda_R}(T)\right], \quad (1)$$

where L is the optical path length (i.e., the geometric thickness of the flame along the optical axis of the imaging system). T is the soot temperature, λ_R=650 nm is the central wavelength corresponding to the R component of the CCD sensor. $\varepsilon_{\lambda_R}(T)$ is the monochromatic emissivity of soot particles at λ_R and T, which can be estimated by [16],

$$\varepsilon_{\lambda_R}(T) = \frac{G(\lambda_R,T)}{G_b(\lambda_R,T)}, \quad (2)$$

where $G(\lambda_R,T)$ and $G_b(\lambda_R,T)$ are the gray-level intensities of the R images of the flame and the blackbody captured by the imaging system at λ_R and T, respectively. The relationship between G_b and T can be determined through the system calibration [6, 14].

Substituting (2) into (1) yields,

$$f_v = -\frac{\lambda_R}{36\pi F(\lambda_R)L}\ln\left(1-\frac{G(\lambda_R,T)}{G_b(\lambda_R,T)}\right), \quad (3)$$

where $F(\lambda_R)$ is a function of complex refraction index and can be expressed as [15],

$$F(\lambda_R) = \frac{nk}{(n^2-k^2+2)^2+4n^2k^2}, \quad (4)$$

where n and k are wavelength dependent real and imaginary parts of the complex refractive index of soot, and can be calculated using empirical equations [16],

$$n = 1.8110+0.1263\ln(\lambda)+0.0270\ln^2(\lambda)+0.0417\ln^3(\lambda), \quad (5)$$

$$k = 0.5821+0.1213\ln(\lambda)+0.2309\ln^2(\lambda)+0.0100\ln^3(\lambda). \quad (6)$$

Note that the soot volume fraction f_v represents the volume of soot per unit volume of gas (ppm). The soot concentration, represented as the value of '$f_v \cdot L$', is also frequently used in the flame measurement [7], which includes information about the optical path length 'L' of the flame.

III. RESULTS AND DISCUSSIONS

Experiments were conducted on a laboratory-scale gas-fired test rig to evaluate the algorithm established for the 3-D reconstruction of the soot volume fraction of flame. Diffusion flames were generated under three different fuel flow rates, i.e., 0.4 l/m, 0.5 l/m, and to 0.6 l/m, with a small air supply to stabilize the flame. For each fuel flow rate, a total of twenty flame images were concurrently captured using the imaging system. The gray-level sections of the flame (i.e., cross- and longitudinal-sections) were then reconstructed, and the soot volume fraction was finally determined using the algorithms as described in section II. Fig. 2(a) shows the overview of the tomographic imaging system and the test rig, whilst Fig.2(b) depicts the typical example 2-D images of flame taken under the fuel rate of 0.5 l/m. The angles given in the figure indicate the angles of view at which the image was taken. It is clear that the shape and gray-level intensity of the flame are different from an angle of view to another, indicating the asymmetric nature of the flame.

Fig. 3 illustrates the reconstructed soot volume fraction distributions of flame cross-sections for the three fuel flow rates. Note that the computed values of the soot volume fraction are normalized by its maximum value over the three test conditions, given a range between 0 and 1. As can be seen, the soot volume fraction is very low and more homogenous in the downstream of the flame (root region, close to the burner outlet) in comparison to other part of the flame. This is attributed to the small amount of air supply which resulted in premixed combustion and thus a lower soot volume fraction in that region.

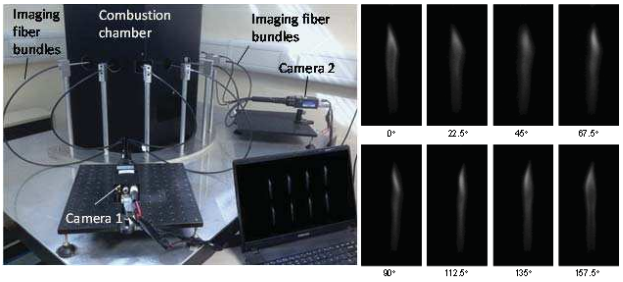

(a) Overview of the imaging system (b) Flame images

Fig. 2. Overview of the tomographic imaging system and flame images taken at eight different angles of view for the fuel rate of 0.5 l/m.

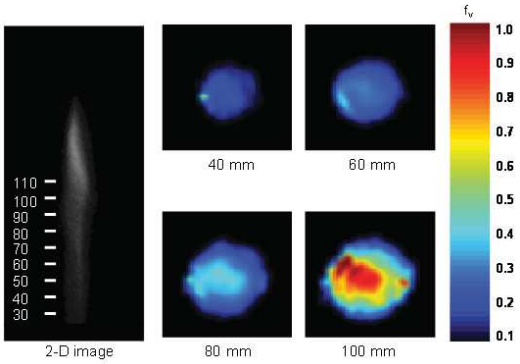

(a) 0.4 l/m

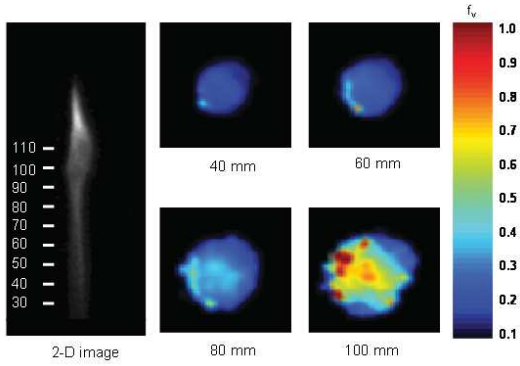

(b) 0.5 l/m

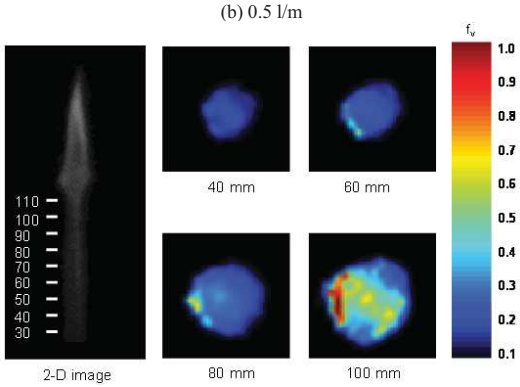

(c) 0.6 l/m

Fig. 3. Soot volume fraction distribution on flame cross-sections for different fuel flow rates.

Fig. 4 illustrates the variations of the mean soot volume fraction along the flame height. It is clear that the soot volume fraction of the flame increases along the flame height and reaches the maximum value at height 120mm for the fuel flow rate of 0.4l/m, 150mm for 0.5l/m, and 160mm 0.6l/m. This is expected for typical diffusion flames. The root part of the flame has particularly a low soot volume fraction due to the small air supply which results in partially premixed combustion and thus reduced soot formation in the region. The standard deviation (STD) of the mean soot volume fraction is also calculated. The maximum normalized STD is 0.38 which occurs at the tip region of the flame (at height 180 mm) under the fuel flow rate 0.6 l/m. This is believed to be attributed to a greater fluctuation in that region, particularly at a higher fuel flow rate.

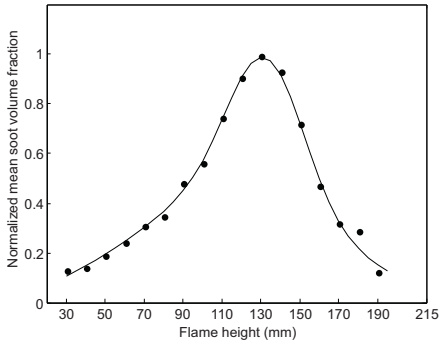

(a) 0.4 l/m

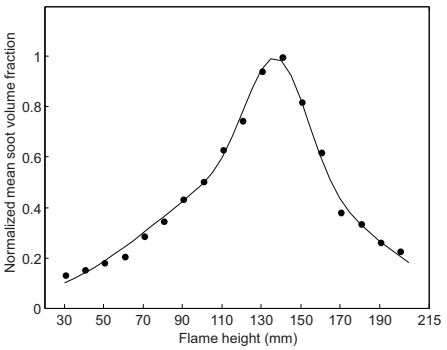

(b) 0.5 l/m

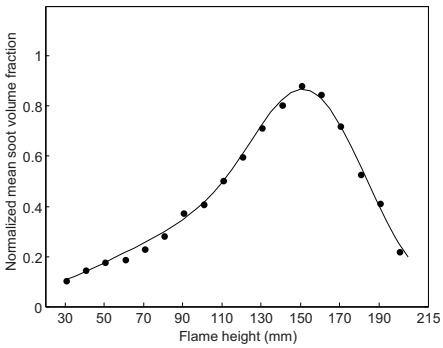

(c) 0.6 l/m

Fig. 4. Variations of the mean soot volume fraction of the flame along the flame height for different fuel flow rates.

The reconstruction of the soot volume fraction can be computed repeatedly for every pixel row of the image along the flame height. Consequently, a large number of cross-sections are obtained that can then be combined to form a complete 3-D reconstructed model of the flame. When this is accomplished, the reconstruction of the longitudinal-sections of flame can be performed. Fig. 5 is the examples of the reconstructed soot volume fraction distribution on longitudinal-sections of flame. It should be noted that the visual representation of the longitudinal-sections depends on the angle of view. The results presented in Fig. 5 show the sections which were viewed at the angle of 0° (refer to the flame images in Fig. 2(b)). Radial distance 0 mm depicts the longitudinal-section along the burner axis, -2 and 2 present the sections about 2 mm backward and forward the burner, respectively, and -4 and 4 present the sections about 4 mm back and forward the burner, respectively. Since those segments are close to the burner axis, they show similar profiles. It has been observed that the root region of each longitudinal-section appears to be very low soot volume fraction for all three test conditions due to the small air supply. It is also found that, for all the fuel flow rates, the soot volume fraction is unevenly distributed over the longitudinal-sections. This may be attributed to the unbalanced fuel and air mixture at the burner outlet.

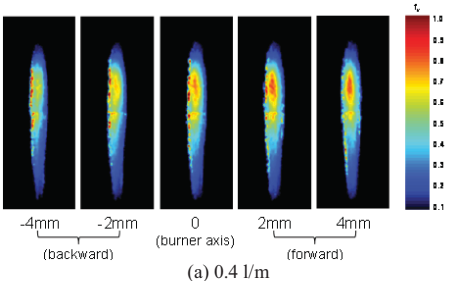

(a) 0.4 l/m

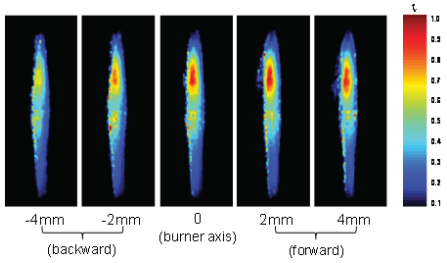

(c) 0.5 l/m

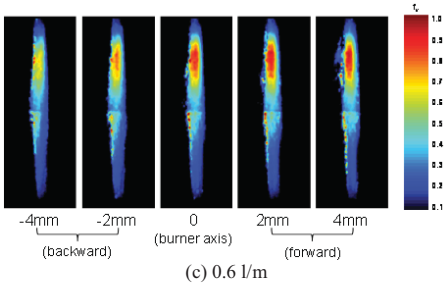

(c) 0.6 l/m

Fig. 5 Soot volume fraction distribution on flame longitudinal-sections under different fuel flow rates.

IV. Conclusions

Tomographic imaging and two-color pyrometric techniques incorporating with the soot radiation theory have been applied for the 3-D reconstruction of the soot volume fraction distribution of asymmetric diffusion flames. 2-D image projections captured at eight different angles of view around the burner have been used for reconstructing the gray-levels of the two primary color images (Red and Green) of flame based on the LFBP-SART algorithm. The distributions of the soot volume fraction of flame have then been determined based on two-color pyrometry and soot radiation theories. Experimental results obtained under three different test conditions have demonstrated the effectiveness of that the proposed technical approach. It has also been evident that the 3-D reconstruction of the flame soot volume fraction distribution can provide very useful information for the in-depth understanding of soot formation mechanisms and subsequent optimization of combustion processes.

References

[1] Z. A. Mansurov, "Soot formation in combustion processes (Review)," *Combustion, Explosion, and Shock Waves*, Vol. 41, No. 6, pp. 727–744, 2005.

[2] C. Lou, C. Chen, Y. P. Sun and H. C. Zhou, "Review of soot measurement in hydrocarbon-air flames", *Sci. China Technol. Sci.*, vol. 53, pp. 2129–2141, 2010.

[3] H. Sapmaz, C. X. Lin and C. Ghenai, "Measurements of soot volume fraction in pulsed diffusion flame by laser induced incandescence," *J. Experiments in Fluids*, vol. 44, pp. 137-144, 2008.

[4] P. Desgroux, X. Mercier, B. Lefort 1, R. Lemaire, E. Therssen and J. F. Pauwels, "Soot volume fraction measurement in low-pressure methane flames by combining laser-induced incandescence and cavity ring-down spectroscopy: Effect of pressure on soot formation," *Combustion and Flame*, vol. 55, pp. 289-301, 2008.

[5] D. R. Snelling, K. A. Thomson, G. J. Smallwood, Ö. L. Gülder, E. J. Weckman and R. A. Fraser, "Spectrally resolved measurement of flame radiation to determine soot temperature and concentration", *AIAA J.*, vol. 40, pp. 1789-1795, 2002.

[6] D. Sun, G. Lu, H. Zhou and Y. Yan, "Measurement of soot temperature, emissivity and concentration of a heavy-oil flame through pyrometric imaging," *Proc. IEEE Int. Instrum Measur. Technol. Conf. (I2MTC 2012),* pp.1865-1869, Graz, Austria, 13-16 May 2012.

[7] H. G. Darabkhani, J. Oakey and Y. Zhang, "Soot concentration and temperature measurements in co-flow laminar propane-air diffusion flames at pressures up to 7 bar," *Proc. 49th AIAA Aerospace Sciences Meeting including the New Horizons Forum and Aerospace Exposition*, AIAA 2011-243, Orlando, Florida, USA, Jan. 4-7, 2011.

[8] Y. Yan, T. Qiu, G. Lu, Md. M. Hossain, G. Gilabert and S. Liu, "Recent advances in flame tomography", *Chinese Journal of Chemical Engineering,* vol. 20, pp. 389-399, 2012.

[9] Md. M. Hossain, G. Lu and Y. Yan, "Optical fiber imaging based tomographic reconstruction of burner flames," *IEEE Trans. Instrum. Meas.*, vol. 61, no. 5, pp. 1417 – 1425, May 2012.

[10] Q. Huang, F. Wang, D. Liu, Z. Ma, J. Yan, Y. Chi and K. Cen,"Reconstruction of soot temperature and volume fraction profiles of an asymmetric flame using stereoscopic tomography," *Combust. Flame*, vol. 156, pp. 565–73, 2009.

[11] S. Veríssimo, T. L. Pedro and A. O. Toledo, "Bi-dimensional reconstruction of a bunsen burner flame," *Proceedings of COBEM 2005 (8th International Congress of Mechanical Engineering)*, Ouro Preto, Brazil, Nov. 6-11, 2005.

[12] G. Legros, P. Joulain, J. P. Vantelon, A. Fuentes, D. Bertheau and J. L. Torero, "Soot volume fraction measurement in a three-dimensional laminar diffusion flame established in microgravity," *Combustion Science and Technology*, vol. 178, pp. 813-835, 2006.

[13] D. Liu, Q. X. Huang, F. Wang, Y. Chi, K. F. Cen and J. H. Yan, "Simultaneous measurement of three-dimensional soot temperature and volume fraction fields in axisymmetric or asymmetric small unconfined flames with CCD cameras," *Journal of Heat Transfer*, vol. 132, pp. 061202-061202, 2010.

[14] Md. M. Hossain, G. Lu. D. Sun and Y. Yan, "Three-dimensional reconstruction of flame temperature and emissivity distribution using optical tomographic and two-colour pyrometric techniques", *Meas. Sci. Technol,* vol. 24(7), doi:10.1088/0957-0233/24/7/074010, 2013.

[15] S. D. Stasio and P. Massoli, "Influence of the soot property uncertainties in temperature and volume-fraction measurements by two-colour pyrometry," *Measurement Science and Technology,* vol. 5, pp. 1453-1465, 1994.

[16] H. Chang and T. T. Charalampopoulos, "Determination of the wavelength dependence of refractive indices of flame soot," *Proc. R. Soc.,* vol. 430, pp. 557–591., 1990.